Human Molecular Genetics, 2010, Vol. 19, No. 14 ***2792–2803***
doi:10.1093/hmg/ddq180
Advance Access published on May 5, 2010

Kidney-specific inactivation of *Ofd1* leads to renal cystic disease associated with upregulation of the mTOR pathway

Alessandro Zullo[1,†], Daniela Iaconis[1,†], Adriano Barra[1], Alessandra Cantone[2], Nadia Messaddeq[4], Giovanbattista Capasso[2], Pascal Dollé[4], Peter Igarashi[5] and Brunella Franco[1,3,*]

[1]Telethon Institute of Genetics and Medicine (TIGEM), via P. Castellino 111, 80131 Naples, Italy, [2]School of Medicine, Second University of Naples, Naples, Italy, [3]Medical Genetics, Department of Pediatrics, Federico II University, Naples, Italy, [4]Institut de Génétique et de Biologie Moléculaire et Cellulaire, BP 10142, 67404 Illkirch Cedex, France and [5]Department of Internal Medicine and Division of Basic Sciences, University of Texas Southwestern Medical Center at Dallas, Dallas, TX, USA

Received February 2, 2010; Revised April 7, 2010; Accepted April 29, 2010

The oral-facial-digital type I syndrome (OFDI; MIM 311200) is a rare syndromic form of inherited renal cystic disease. It is transmitted as an X-linked dominant, male lethal disorder and is caused by mutations in the *OFD1* gene. Previous studies demonstrated that OFDI belongs to the growing number of disorders ascribed to dysfunction of primary cilia. We generated a conditional inactivation of the mouse *Ofd1* gene using the *Ksp-Cre* transgenic line, which resulted in a viable model characterized by renal cystic disease and progressive impairment of renal function. The study of this model allowed us to demonstrate that primary cilia initially form and then disappear after the development of cysts, suggesting that the absence of primary cilia is a consequence rather than the primary cause of renal cystic disease. Immunofluorescence and western blotting analysis revealed upregulation of the mTOR pathway in both dilated and non-dilated renal structures. Treatment with rapamycin, a specific inhibitor of the mTOR pathway, resulted in a significant reduction in the number and size of renal cysts and a decrease in the cystic index compared with untreated mutant animals, suggesting that dysregulation of this pathway in our model is mTOR-dependent. The animal model we have generated could thus represent a valuable tool to understand the molecular link between mTOR and cyst development, and eventually to the identification of novel drug targets for renal cystic disease.

INTRODUCTION

Oral-facial-digital syndrome type I (OFDI; MIM 311200) is a rare developmental disorder ascribed to ciliary dysfunction and inherited as an X-linked dominant condition with lethality in males. It is characterized by malformations of the face, oral cavity and digits and renal cystic disease (1), which in many cases completely dominates the clinical course of the disease (2,3). Recent data revealed that renal cystic disease is present in over 63% of adult cases (>18 years), indicating that cystic kidney disease is more frequent than previously estimated in this condition (4). Histochemical analysis of cystic renal tissues from OFDI patients demonstrate a predominantly glomerulocystic kidney disease with a minor population of cysts derived from distal tubules (3). As in other inherited forms of polycystic kidney disease (PKD), cysts in other organs, such as pancreas, ovary and liver, have also been reported in OFDI patients (5–7).

The gene responsible for this genetic disorder, named *OFD1*, encodes a 1011-amino acid protein localized to the centrosome (8) and the basal body at the base of primary cilia in most cells, including fully differentiated renal epithelial cells (9,10). We previously generated Ofd1-knockout mice (11). Heterozygous females reproduced the main features

*To whom correspondence should be addressed. Tel: +39 0816132207; Fax: +39 0816132351; Email: franco@tigem.it
†The authors wish it to be known that, in their opinion, the first two authors should be regarded as joint First Authors.

of the human disease and displayed severe craniofacial abnormalities, limb and skeletal defects and cystic kidneys. Immunofluorescence and scanning electron microscopy (SEM) studies demonstrated the absence of cilia on the luminal surfaces of cells that lined the cysts, thus implicating ciliogenesis as a mechanism underlying cyst development in OFDI. SEM studies also demonstrated lack of nodal cilia in the embryonic node of hemizygous males, leading to laterality defects. These results definitively placed OFD type I in the growing number of disorders associated with ciliary dysfunction and indicate that Ofd1 is required for primary cilia formation and left–right axis specification (11).

An increasing amount of data suggest a possible correlation between the cystic disease and the dysfunction of primary cilia in renal cells. Cilia dysfunction might lead to a wide spectrum of syndromic disorders such as Bardet–Biedl syndromes (BBS), Joubert, Meckel and OFD type I syndromes, which are all characterized by the presence of cystic kidneys associated with additional clinical signs (12–14). Interestingly, most of the protein products encoded by the genes responsible for inherited forms of PKD, such as autosomal dominant (ADPKD) and autosomal recessive polycystic kidney diseases and nephronophthisis (NPHP), are all expressed in primary cilia, basal bodies or centrosomes, suggesting that ciliary dysfunction might be the unifying pathogenic mechanism underlying cystic kidney disease (15–17). However, the underlying molecular mechanisms remain undetermined, and it is still not clear whether ciliary dysfunction is the primary event underlying renal cysts formation.

Much effort has been directed to find a common pathway that could explain cystogenesis in the different types of PKD disorders. Several molecular pathways have been involved, but deregulation of cell growth is an extremely common, if not universal, feature of this phenomenon (18). Recent data indicate that the mTOR pathway could play an important role in renal cysts formation, and it has been shown that an inhibitor of mTOR, rapamycin, slows disease progression (19–22).

Here, we present a conditional model in which *Ofd1* was specifically inactivated in the kidney. We show that cilia are present in precystic tubules and disappear after the formation of cysts, suggesting that the absence of cilia is consequent to the development of cysts. In these animals, we also demonstrate abnormalities in cell proliferation, upregulation of the mTOR pathway and a significant reduction in renal cysts upon administration of rapamycin.

RESULTS

Generation of a conditional model with *Ofd1* kidney-specific inactivation

To overcome the problem of embryonic male and perinatal female lethality observed in *Ofd1* knockout ($Ofd1^{\Delta 4-5}$ and $Ofd1^{\Delta 4-5/+}$) mutant animals (11), we generated a mouse line with kidney-specific inactivation of *Ofd1* by crossing females from the *Ofd1*-floxed line ($Ofd1^{fl}$) with the *Ksp-Cre* transgenic line in which cre recombinase is specifically expressed in renal tubular epithelial cells and the developing genitourinary tract under the control of the Ksp-cadherin (Cdh16) gene promoter (23). The resulting mice, both females ($Ofd1^{fl/+}$;cre^{Ksp}) and males ($Ofd1^{fl/y}$;cre^{Ksp}), were viable and indistinguishable from wild-type (wt) animals. RT–PCR analysis of these genotypes confirmed the kidney-specific inactivation of *Ofd1*. This analysis revealed that the mutated allele is present only in the kidney of mutant animals, whereas it is absent in other organs, such as the lung, where only the wt allele could be detected (Fig. 1A). To determine more accurately the extent of *Ofd1* inactivation, we performed quantitative RT–PCR with primers that specifically amplify the wt *Ofd1* allele on genomic DNA (primers B and B′ in Fig. 1B) and on RNA (primers A and A′ in Fig. 1B) obtained from kidneys of $Ofd1^{fl}$;cre^{Ksp}-conditional mutants and controls. Primers A′ and B′ do not anneal on the deleted allele, thus allowing to specifically amplify the wt allele. Our analysis revealed the presence of 40 and 30% of the mutated allele on genomic DNA of whole kidneys from $Ofd1^{fl/y}$;cre^{Ksp} and $Ofd1^{fl/+}$;cre^{Ksp} mutants, respectively, when compared with controls. Similar results were obtained by analysis of the RNA (Fig. 1B). The incomplete inactivation of Ofd1 in the kidneys of $Ofd1^{fl}$;cre^{Ksp} animals was expected since cre recombinase is not expressed in all renal cells; however, one cannot exclude an incomplete efficiency of cre/loxP recombination (23).

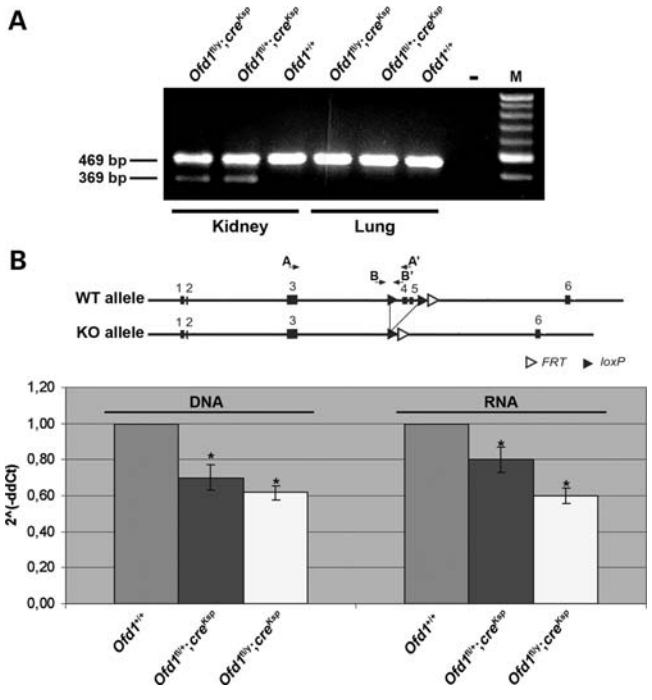

Figure 1. *Ofd1* inactivation in mutant animals. (**A**) RT–PCR analysis showed the presence of the mutant $Ofd1^{\Delta 4\text{-}5}$ allele (369 bp) only in the kidney of $Ofd1^{fl/y}$;cre^{Ksp} and $Ofd1^{fl/+}$;cre^{Ksp} mutant animals. The mutated allele is absent in the lung of mutants and in the kidney and lung of wt ($Ofd1^{+/+}$) mice. All samples showed the presence of the wt allele (469 bp). No amplification was observed in the negative control. M = marker. (**B**) Quantitative RT–PCR with primers that specifically amplified the wt *Ofd1* allele on genomic DNA (primers A and A′) and on RNA (primers B and B′). The position of the primers is displayed in the upper scheme. The analysis was performed on genomic DNA and RNA from kidneys of conditional mutants ($Ofd1^{fl/y}$;cre^{Ksp}, $Ofd1^{fl/+}$;cre^{Ksp}) and controls ($Ofd1^{+/+}$). Significant differences between mutants and controls ($P < 0.05$) are indicated (asterisk). Error bars represent standard error of the mean.

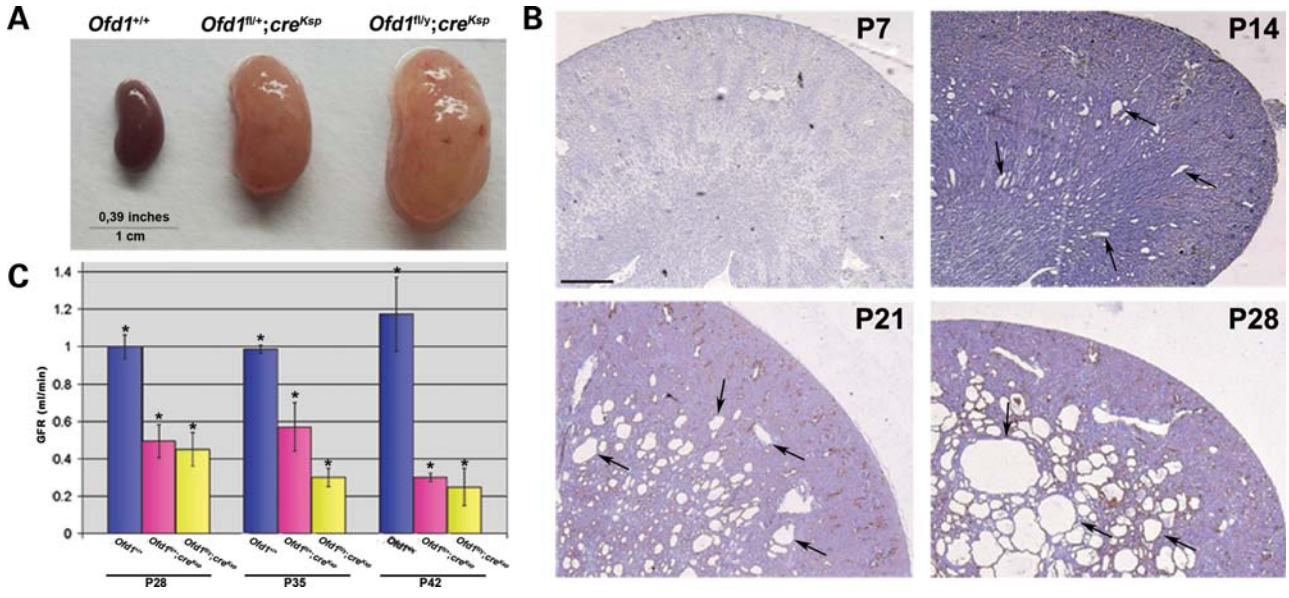

Figure 2. Characterization of Ofd1 mutant animals. (**A**) Gross appearance of kidneys from *Ofd1*$^{+/+}$ (left), *Ofd1*$^{fl/+}$;*cre*^{Ksp} (center) and *Ofd1*$^{fl/y}$;cre^{Ksp} (right) mice at P70. (**B**) Hematoxylin/eosin staining of kidneys sections from *Ofd1*$^{fl/y}$;*cre*^{Ksp} mutants at different stages. At P7, no cysts are visible. Dilated tubules appeared at P14 and cysts (black arrows), rapidly increased in size and number. Bar = 500 μm. (**C**) GFR at different stages showed a reduced renal function in the kidney from mutant males (*Ofd1*$^{fl/y}$;*cre*^{Ksp}) and females (*Ofd1*$^{fl/+}$;*cre*^{Ksp}) compared with control littermates (*Ofd1*$^{+/+}$). Bars = standard error of the mean. Data were analyzed by Student's *t*-test. $^{*}P < 0.05$.

Cysts progression, abnormal renal function and origin of cysts in *Ofd1* mutants

We have previously shown that kidneys of *Ofd1*$^{\Delta 4-5/+}$ female mutants, in which the *Ofd1* transcript is inactivated at the four-cell stage, display renal cysts at P0 (11). A more detailed study of these animals revealed the presence of glomerular cysts starting from E14.5 (data not shown). Interestingly, we never observed cysts of tubular origin in these animals.

Ofd1^{fl};*cre*^{Ksp} mice were born at the expected Mendelian ratio and did not show gross abnormalities. By P70, the animals were characterized by an enlargement of the abdomen, which was more evident in male mutants, and lethargy. At this stage, the parenchyma of mutant kidneys was considerably enlarged (Fig. 2A). In *Ofd1*$^{fl/y}$;*cre*^{Ksp} males, renal cysts were not observed at P7, whereas dilated tubules were visible starting from P14, after which cysts became larger and more numerous (Fig. 2B). By P35, we observed a massive replacement of the renal parenchyma by cysts (data not shown). Histological examination revealed that cysts progression in *Ofd1*$^{fl/+}$;*cre*^{Ksp} female mutants was similar, although the number of cysts observed was reduced, probably owing to the X- inactivation phenomenon. Cysts were confined to the medullary portion of the kidney up to P28. Starting from P35, cysts appear in the kidney cortex (data not shown), where expression of Ksp-cadherin has been detected at adult stages (23). At P70, glomerular cysts were also observed (data not shown), as reported in other conditional models obtained using the *Ksp-Cre* line (24,25). The renal function of *Ofd1*^{fl};*cre*^{Ksp} mutants was assessed by analysis of the glomerular filtration rate (GFR) starting from P28. At this stage, a marked reduction of the GFR was observed in both male and female mutants, indicating a severe impairment of the renal function. GFR analysis at later stages indicated a progressive deterioration of the renal function (Fig. 2C). We observed mutants up to P90. After this stage, mutant animals were sacrificed.

To establish the cellular origin of cysts, we performed staining with antibodies or lectins that specifically label different segments of the nephron, and the results of this study are shown in Figure 3. The cysts were preferentially labeled with the antibody against the Tamm–Horsfall protein (THP), which labels the thick ascending limb of Henle's loop, although some cysts were positive for *Arachis hypogaea* lectin, which labels distal tubules and collecting ducts. Staining with an antibody to the Na-PiII (NaPiII) transporter, which marks the proximal tubules, did not label any cysts until P28. Taken together, these results indicated a primarily distal tubular origin of the cysts. Staining with Na-PiII confirmed the presence of proximal cysts at P35 (data not shown). Staining with periodic acid-Schiff (PAS) allowed us to exclude the presence of fibrosis in mutant kidneys.

Primary cilia are present on renal epithelial cells in a precystic stage

To evaluate the effect of *Ofd1* inactivation on cilia formation in renal cells, we performed staining with an anti-acetylated tubulin antibody that labels the axoneme of primary cilia. At P0 (data not shown) and P7, immunofluorescence analysis showed that cilia were present in all tubules of mutant kidneys, indicating that cilia form at precystic stages (arrowheads in Fig. 4B and C). At P14, when cysts can be detected, no cilia protruding from cells lining the renal cysts were detected in both female and male mutants (Cy in Fig. 4H and I), whereas cilia were present in non-cystic distal tubules from the same animals (arrowheads in Fig. 4H and I).

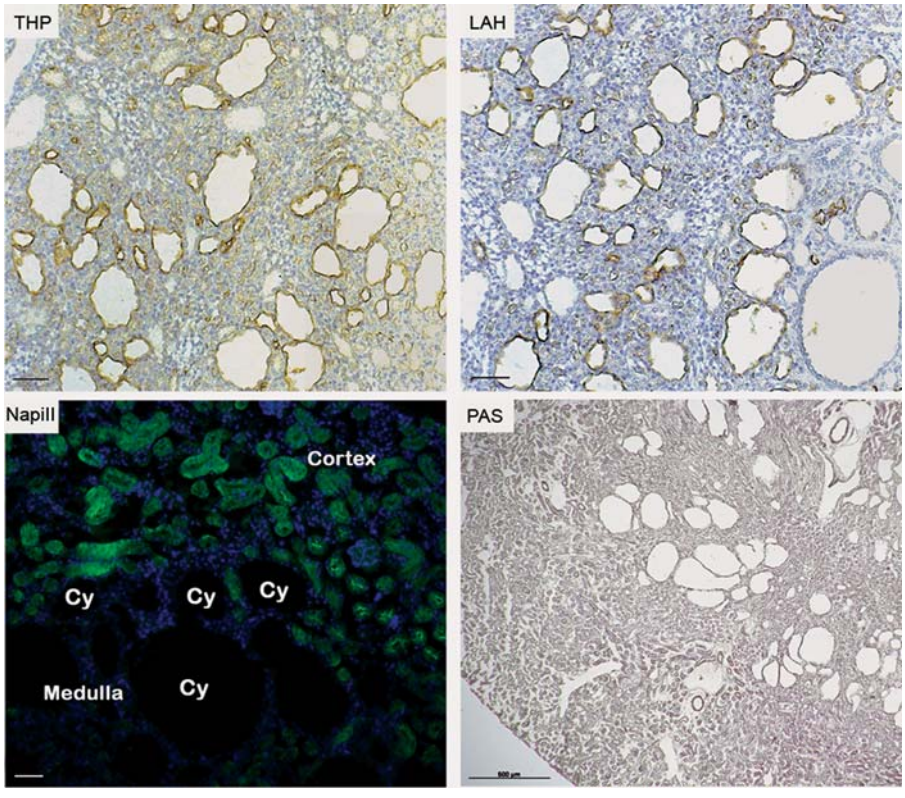

Figure 3. Cysts origin in *Ofd1*$^{fl/y}$;*cre*^{Ksp} mutant animals. Kidneys from *Ofd1*$^{fl/y}$;*cre*^{Ksp} mutants at P21 were stained for Tamm–Horsfall protein (THP), *Arachis hypogaea* lectin (LAH) and Na-PiII co-transporter (green, NaPiII). The cysts were positive for THP and LAH, thus indicating a distal tubular origin of cysts. Na-PiII transporter, a marker of proximal tubules, did not label any cysts (Cy) at this stage. Nuclei were counterstained with 4′,6-diamidino-2-phenylindole (DAPI, blue). PAS staining on kidneys from *Ofd1*$^{fl/y}$;*cre*^{Ksp} excluded the presence of fibrosis. Bar = 50 μm for THP, LAH and NapiII panels. Bar = 500 μm for PAS staining.

To confirm this observation, we performed SEM analysis on wt and mutant animals (one female and two male mutants). Five different slices were analyzed for each animal for a total of approximately 100 cells observed for wt and female mutant and >200 for the male mutants. This study revealed that at P0 (data not shown) and P7, the majority of the cells examined in all animals (>95%), regardless of the genotype, showed the presence of cilia (arrows in Fig. 4D–F). Conversely, at P14, cilia were absent from the dilated tubules of mutant kidneys (Fig. 4M and N), whereas ciliated structures could be detected in wt kidney (arrow in Fig. 4L).

To verify whether ciliated cells expressed the Cre recombinase at precystic stages, we performed immunofluorescence analysis with an anti-acetylated tubulin antibody and an antibody recognizing the Cre protein. Our results indicate that at precystic stages, cells expressing the Cre recombinase displayed primary cilia (arrows in Supplementary Material, Fig. S1).

Taken together, these data indicate that cilia initially formed in the absence of Ofd1 and were then subsequently lost after cyst formation.

Upregulation of mTOR pathway in *Ofd1*^{fl};*cre*^{Ksp} mutant kidneys

Several lines of evidence link the mTOR pathway to cell proliferation and cystic kidney disease (19,26). To test a possible alteration of this pathway in *Ofd1*^{fl};*cre*^{Ksp} mutants, we initially performed immunofluorescence experiments using an antibody against the phospho-S6 ribosomal protein (P-S6), which is considered a read-out of the mTOR pathway. This study revealed a diffuse activation of S6 in mutant kidneys, which was more evident in the cells surrounding the cysts, thus suggesting an abnormal activation of the mTOR pathway (Fig. 5A–G). Interestingly, dysregulation of the mTOR pathway was also observed in non-dilated tubules, suggesting that the upregulation of this pathway precedes cyst formation (arrowheads in Fig. 5D and G). Moreover, it should also be noted that not all cysts display upregulation of the mTOR pathway (asterisks in Fig. 5D and F). As a control, we performed immunofluorescence analysis using both an antibody recognizing the Cre protein and the antibody against P-S6. Our study demonstrated that the majority of the cells positive for P-S6 (green) also express the Cre recombinase (red) in mutant animals as shown in Supplementary Material, Figure S2 (merge in B and C). This result further strengthens the link between the upregulation of the mTOR pathway and the absence of *Ofd1*. We then looked at both the phosphorylation state and the expression levels of S6 by western blotting analysis. This study revealed an increase in the amount of P-S6 in *Ofd1*^{fl};*cre*^{Ksp} mutant kidneys from both male and female mutant animals (Fig. 5H, top panel), whereas no changes in the total amount of S6 protein were detected (Fig. 5H, bottom panel). This result further supports an increased activation of the mTOR pathway in animals

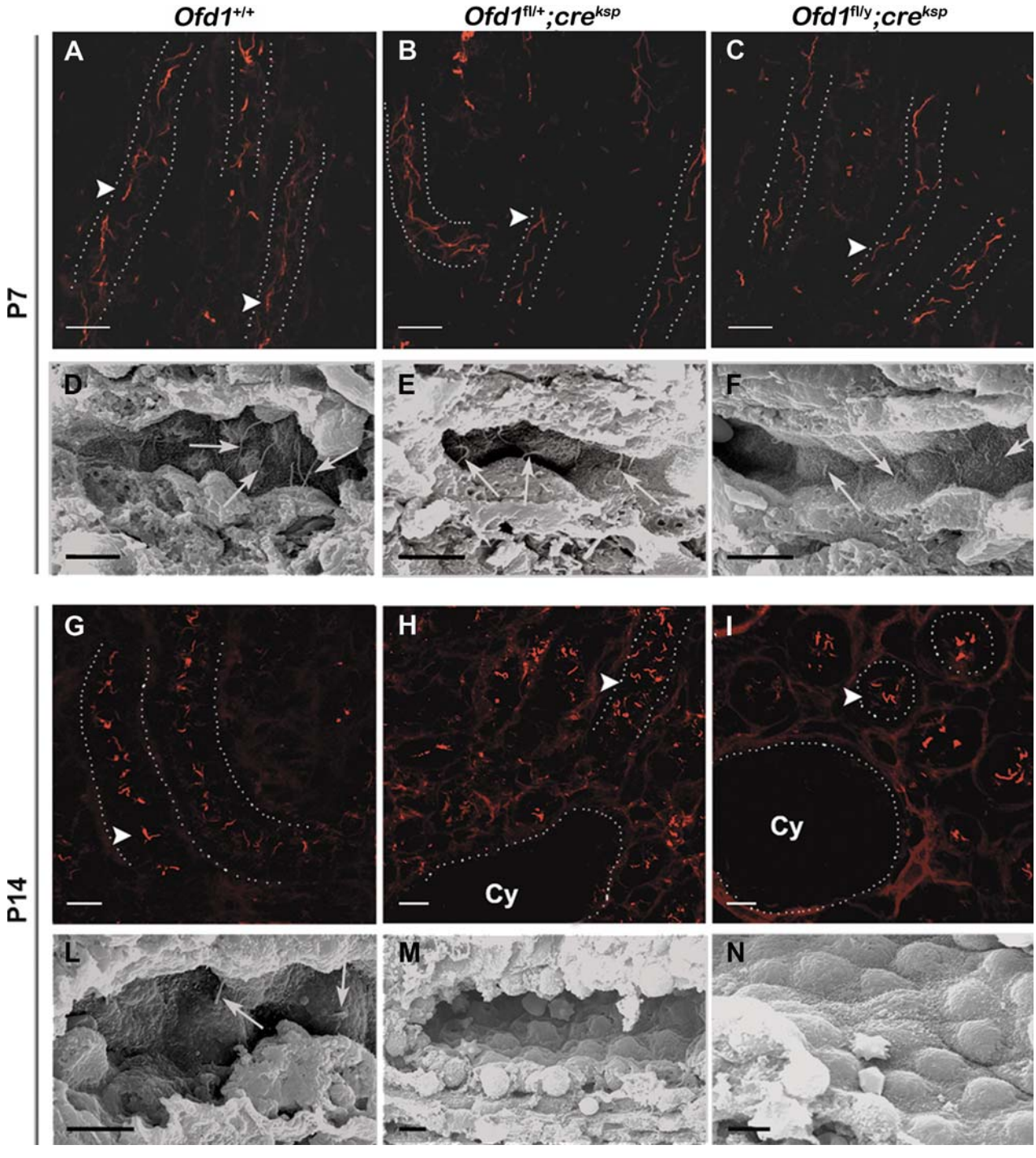

Figure 4. Analysis of primary cilia in renal tubules of *Ofd1*^{fl};*cre*^{Ksp} mutant animals. Immunostaining with anti-acetylated tubulin (red) and SEM analysis revealed the presence of cilia in *Ofd1*^{fl};*cre*^{Ksp} and control littermates (*Ofd1*$^{+/+}$) at P7 in the kidney distal tubules [arrowheads in (**A**–**C**), arrows in (**D**–**F**)]. Immunostaining with anti-acetylated tubulin (red) showed the absence of cilia in the cells lining the cysts (Cy) and the presence of cilia in non-dilated tubules (arrowheads) from *Ofd1*$^{fl/+}$;*cre*^{Ksp} (**H**) and *Ofd1*$^{fl/y}$;*cre*^{Ksp} (**I**) mutants at P14. Cilia are normally seen in *Ofd1*$^{+/+}$ control animals (**G**). SEM analysis confirm the absence of cilia from cells lining cystic dilations in both *Ofd1*$^{fl/+}$;*cre*^{Ksp} (**M**) and *Ofd1*$^{fl/y}$;*cre*^{Ksp} (**N**) mutants at P14, whereas cilia are present in control littermates at the same stage (arrows in **L**). Bars = 10 μm (A–C, G–I); 5 μm (D–F, L–N). Tubules are outlined with dotted lines.

carrying inactivation of the *Ofd1* transcript. Western blotting analysis with antibodies recognizing other key molecules (AKT, mTOR, P70S6K) did not detect any changes for what concerns the state of phosphorylation and the total amounts of other proteins involved in the AKT/mTOR pathway (Supplementary Material, Fig. S3).

Since mTOR is involved in cell proliferation, we performed staining with an anti-PCNA antibody in wt and mutant kidneys

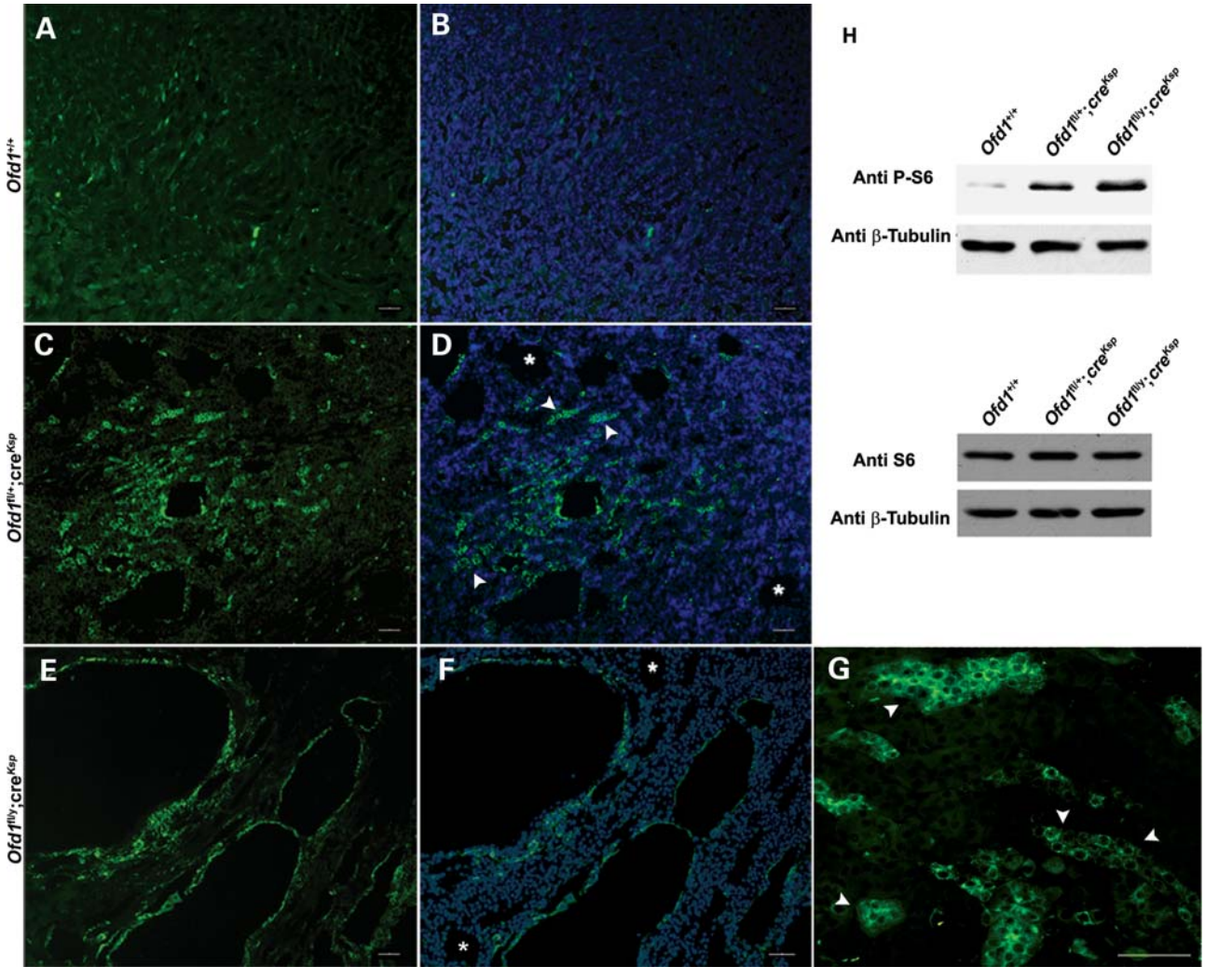

Figure 5. Upregulation of the mTOR pathway in *Ofd1*^{fl};*cre*^{Ksp} mutant animals at P21. Immunostaining and western blot analysis with anti-phospho S6 (P-S6). The immunofluorescence revealed an higher level of P-S6 (green) on kidney sections from *Ofd1*$^{fl/+}$;*cre*^{Ksp} (**C** and **D**) and *Ofd1*$^{fl/y}$;*cre*^{Ksp} (**E**–**G**) mutant animals when compared with *Ofd1*$^{+/+}$ controls (**A** and **B**). In (B), (D) and (F), nuclei were counterstained with DAPI (blue). Fews cysts do not display staining with anti P-S6 (asterisks in D and F). Upregulation of P-S6 (arrowheads) is observed also in non-dilated tubules in both *Ofd1*$^{fl/+}$;*cre*^{Ksp} (D) and *Ofd1*$^{fl/y}$;*cre*^{Ksp} (magnification in G) mutant animals. Bars (A–G) = 50 μm. (**H**) Western blot analysis of total S6 (lower panel) and P-S6 (upper panel) on total protein extracts of kidneys from *Ofd1*$^{+/+}$, *Ofd1*$^{fl/+}$;*cre*^{Ksp} and *Ofd1*$^{fl/y}$;*cre*^{Ksp} animals confirmed the upregulation of the mTOR pathway.

at P14. We observed a marked increase in proliferating cells in mutant kidneys compared with wt (Supplementary Material, Fig. S4). The same result was observed at later stages (P21 and P28, data not shown). Staining with the anti-cleaved Caspase-3 antibody also revealed a moderate increase in apoptotic cells in the epithelial layer lining the cysts (data not shown).

In addition, to further address the nature of the upregulation of this pathway, we transfected Madin–Darby canine kidney cells (MDCK) with siRNAs against the canine *OFD1* and measured P-S6 levels. Interestingly, the phosphorylated form of the S6 protein was increased in *OFD1* siRNA-treated MDCK cells 48 h after transfection (Supplementary Material, Fig. S5A), when the *OFD1* transcript levels decrease by 60% (Supplementary Material, Fig. S5B), whereas no changes were observed in scrambled siRNA-treated cells. These results suggest that the upregulation of mTOR is not a secondary event and is directly linked to the *OFD1* inactivation.

Inhibition of mTOR pathway reduces cystogenesis in *Ofd1*^{fl};*cre*^{Ksp}

To further evaluate the role of Ofd1 in mTOR signaling, mutant *Ofd1*^{fl};*cre*^{Ksp} mice and control littermates were treated with rapamycin, a specific inhibitor of the mTOR pathway (27), starting at P14, when the renal cysts appear in our conditional knockout model. After 10 days of treatment, animals were sacrificed at P24 and analyzed. Histological analysis of rapamycin-treated mutant mice showed a clear reduction in the number and size of cysts compared with non-treated mutant animals (Fig. 6A and B). Hematoxylin–eosin analysis revealed a normal structure of kidneys in control mice treated with rapamycin (Fig. 6C). We also calculated the cystic index and showed that it is significantly reduced in rapamycin-treated mutant mice, confirming that the rapamycin treatment does indeed slow cysts progression

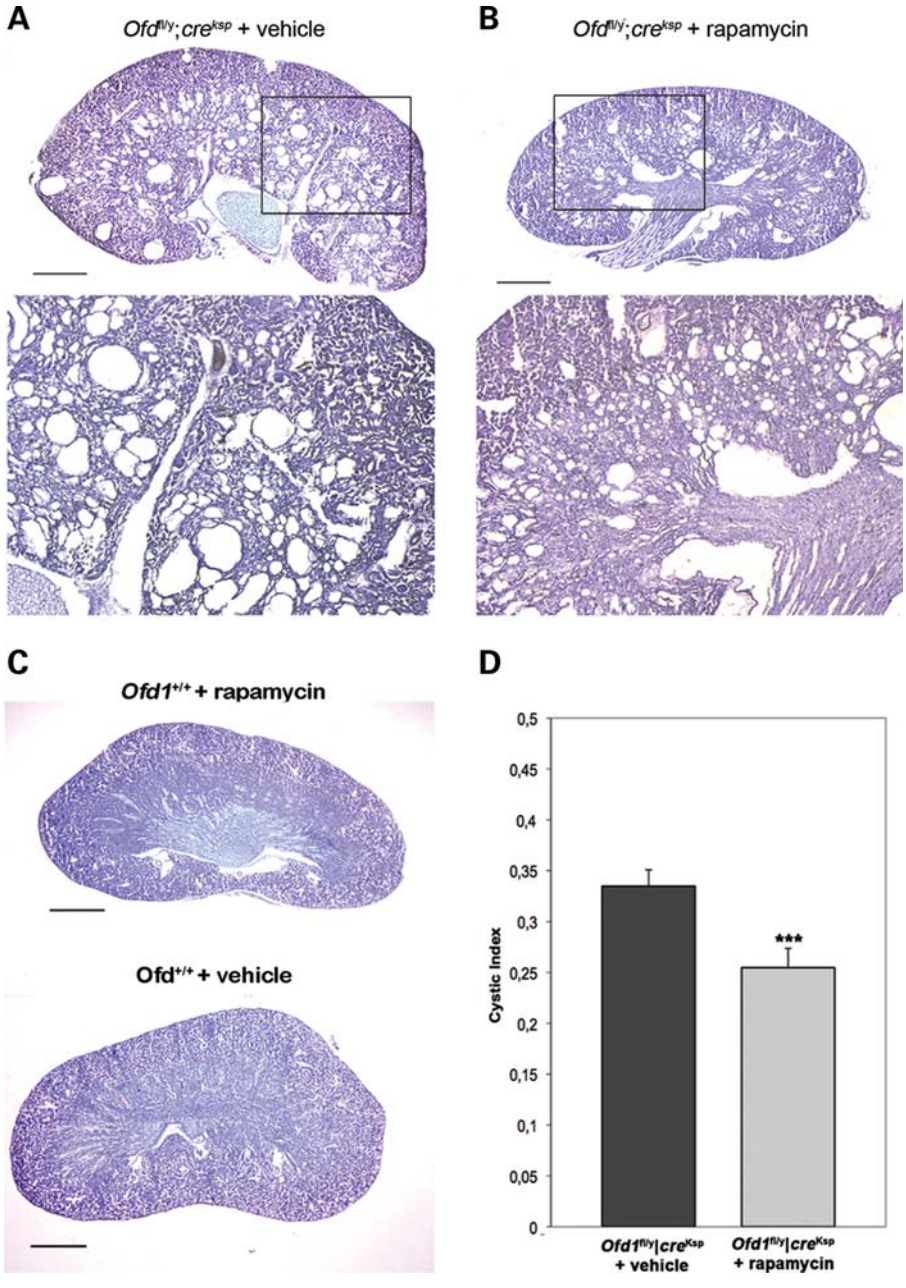

Figure 6. Rapamycin treatment significantly improves the renal cystic phenotype observed in *Ofd1*$^{fl/y}$;*cre*^{Ksp} animals (**B**) when compared with mutant animals treated with vehicle alone (**A**). Bottom panels in (A) and (B) represent higher magnification of the boxed images. In (**C**), kidneys from wt littermates treated with rapamycin or vehicle alone are shown as a control. (**D**) Cystic indices were calculated based on representative renal sections from non-treated and treated *Ofd1*$^{fl/y}$;*cre*^{Ksp} mice ($n = 3$ kidneys). Bars in (A), (B) and (C) = 1.2 mm. Data were analyzed by Student's *t*-test. $^{***}P < 0.005$.

(Fig. 6D). Taken together, these results suggest that cystogenesis in our mouse model is mTOR-dependent.

DISCUSSION

A new model for inherited PKD

We demonstrated that *Ofd1*$^{\Delta 4-5/+}$ heterozygous females develop glomerular cysts as early as E14.5. In this study, we show that kidney-specific inactivation of *Ofd1* leads to viable mice that develop cysts of tubular origin starting from P14. The *Ksp-Cre* line used in this study is expressed starting from E15.5 in the kidney specifically and its expression is predominantly in the medullary portion of the kidney. Accordingly, the conditional model we generated displays cysts originating from distal segments of the nephron. These results allow us to draw two conclusions: (i) the *Ofd1* transcript is important from the early stages of renal development and (ii) *Ofd1* inactivation can lead to cystic dilation of both tubular and glomerular structures. To date, we never observed cysts of tubular origin in *Ofd1*$^{\Delta 4-5}$ mutant females. OFDI patients display a prevalence of glomerulocystic kidney

disease with a minor population of cysts from distal tubules (3). It is conceivable that glomeruli are more sensitive to *Ofd1* deficiency, leading to the early appearance of glomerular cysts in $Ofd1^{\Delta 4-5}$ females and to the predominance of cysts of glomerular origin in OFDI patients. Unfortunately, owing to the perinatal female lethality, we cannot analyze $Ofd1^{\Delta 4-5}$ females at more advanced stages to verify whether tubular cysts will develop at later stages in this model. Taken together, our data suggest that *Ofd1* is important in all segments of the nephron and the availability of both murine models will be critical to evaluate the role of Ofd1 in the formation of cysts in the different structures.

Interestingly, in the $Ofd1^{fl}$;cre^{Ksp} mutants, we also observed at later stages glomerular cysts, and it is well established that the Ksp transcript is not expressed in glomerular structures (23). The same observation has been reported for the *Ksp-Cre;Hnf1*$\beta^{flox/flox}$ mutants (25), whereas no glomerular cysts were observed in the $Pkd1^{flox/-}$:*Ksp-Cre* animals (28). These results suggest that the glomerular cysts in these models may be the product of secondary cystogenetic events which appear to take place only when specific transcripts are inactivated.

Different animal models for PKD have been generated, although with great variability in the stage and site of occurrence of renal cysts. These differences are partly due to the use of different cre lines, different genetic backgrounds of the murine models and to the specific role, site and timing of expression of the genes to be inactivated. However, recent data identify a crucial 2-day interval (from P12 to P14) in renal maturation (29). As a consequence, inducible inactivation of *Pkd1* in the mouse at different time points resulted in a very different disease progression (29,30). On the basis of these observations, we cannot exclude a specific role of the *Ofd1* transcript in renal development around P13–P14, when we observe the first dilatation of tubules in the $Ofd1^{fl}$;cre^{Ksp} model.

Primary cilia disappear after cyst formation in *Ofd1* conditional mutants

The list of ciliary proteins involved in PKD continues to grow, as well as the number of animal models in which the presence of renal cysts is associated to cilia dysfunction (15,31). Despite this observation, it should be noted that there are a few reports of animal models in which inactivation of ciliary proteins results in cystic kidneys in which primary cilia remain present, although no data are available on the functionality of these cilia (32,33). Therefore, although the connection between primary cilium and renal cystic disease is evident, there is no clear demonstration of a direct, causal relationship between ciliary dysfunction and cyst formation. It is important to keep in mind that most cystoproteins are not exclusively localized to the cilia. For example, polycystin-1, nephrocystin and inversin, which are the proteins encoded by the genes responsible for ADPKD, NPHP1 and NPHP2, respectively, have also been detected in other cellular structures (18,34–36) and are involved in cell–cell and cell–matrix interactions. We recently reported that OFD1 is not exclusively localized to the centrosome and basal body, but is present also in the nucleus (10). Impairment of the function of OFD1 in either of these subcellular compartments could independently result in altered tubular morphology leading to renal cysts formation. One challenge that remains to be addressed is to separate the cilia-specific function and properties of the various proteins from other functions/roles that they might have in the cell. The studies of the different murine models carrying inactivation of the Ift88 protein (also known as Tg737 or polaris) are particularly informative in this regard. Ift88 is a ciliary protein that is crucial for intraflagellar transport and cilium assembly (37,38). Mice lacking Ift88 die at mid-gestation, display absence of nodal cilia and exhibit neural tube and situs inversus (39). Mice homozygous for a hypomorphic allele named *orpk* survive to birth and have cystic kidney disease associated with the presence of stunted and malformed cilia (40,41). Unexpectedly, transgenic overexpression of Ift88 in a null TgN737 background results in mice with normal nodal function and renal cystic disease with cilia of normal length and morphology, thus indicating a partial rescue of the functions associated with cilia (42,43). Altogether, these results suggest that, in these models, ciliary dysfunction does not fully explain renal cystogenesis.

In addition, it is also known that non-ciliary proteins give rise to renal cystic disease when mutated. In particular Bicaudal C is a conserved RNA-binding protein that is mutated in two murine models for renal cystic disease, the *jcpk* and *bpk* models (44). However, recent findings link the activity of this RNA-binding protein with the orientation of cilia via Wnt signaling (45). Another example is the FLCN protein, also known as folliculin. Mutations in the *BHD/FLCN* gene cause the Birt–Hogg–Dube syndrome characterized by renal cystic disease and increased risk for renal neoplasia. The gene product localizes to the cytoplasm and the nucleus and seems to be involved in the regulation of the mTOR pathway (46–48).

We have now demonstrated that, in renal epithelial cells devoid of *Ofd1*, primary cilia are present prior to the formation of renal cysts and then are subsequently lost. Interestingly, the same observation was reported for a conditional mouse model with a *Kif3A* kidney-specific inactivation (49). To date, we do not know whether these cilia function normally and further experiments are needed to address this question. Our data confirm the association between primary cilia and renal cystic disease, and we propose that in our model the development of renal cysts might not be a direct consequence of the loss of cilia. Unfortunately, no data are available concerning the presence of cilia in precystic stages in other models for PKD, and it is difficult to assess whether this hypothesis can be generally applied or is specific to the renal cystic disease resulting from *Ofd1* inactivation.

Upregulation of the mTOR pathway in $Ofd1^{fl}$;cre^{Ksp} mutants

We demonstrated an upregulation of the phospho-S6 molecule in both dilated and non-dilated tubules in the kidneys of $Ofd1^{fl}$;cre^{Ksp} mutants. A possible role of mTOR in renal cystic disease is supported by recent reports indicating that rapamycin, an inhibitor of mTOR, slows down cyst progression in different animal models, suggesting that the mTOR pathway is a converging point in the cystogenesis

(19–22). However, it is still not clear if the activation of the mTOR pathway is the cause of cyst development. Different studies, including our report, have shown that not all renal cysts, in ADPKD patients as well as in mouse mutants, show upregulation of the mTOR pathway, suggesting that this pathway could be involved in cyst expansion rather than cyst formation (26).

The mTOR pathway has also been implicated in tuberous sclerosis (TSC), a tumor suppressor gene syndrome associated with renal cystic disease. The proteins encoded by the *TSC1* and *TSC2* genes, hamartin and tuberin, respectively, physically interact with each other inhibiting the mTOR pathway (50–52). Recent findings obtained in a murine model, generated by conditional deletion of the *Tsc1* gene in a subset of renal tubular cells, indicate that the loss of *Tsc1* causes renal cystic disease by activation of the mTOR pathway (53). In addition, it was recently demonstrated that knockdown of one of the *TSC1* zebrafish homologs leads to renal cystic disease with upregulation of the mTOR pathway in the cells that line renal cysts, and to the presence of longer cilia in the otic vesicle and pronephric ducts from morphants (54). Moreover, mouse embryonic fibroblasts from $Tsc1^{-/-}$ and $Tsc2^{-/-}$ mutants show an increased number of cilia, which is not rescued by treatment with rapamycin, suggesting that the enhanced cilia formation is mTOR-independent (55). These data underline the link between the mTOR pathway, cilia and renal cysts, even if they do not clarify the role of cilia in the mTOR-dependent mechanisms leading to cyst pathogenesis. In our model, we show, for the first time, that the upregulation of the mTOR pathway is evident also in non-dilated tubules where cilia appear to be present. In addition, as discussed above, there is accumulating evidence that ciliary proteins have other functions in the cells and that renal cysts can also be linked to non-ciliary proteins. These observations suggest that the activation of mTOR can occur before cyst development and that this event could determine tubules dilation. The persistent activation of the pathway in a portion of the cysts might contribute to the increase in the size of the cysts (26).

The mTOR pathway has essential roles in protein translation, cell growth and proliferation, and is upregulated in several types of tumors. It represents a potentially interesting therapeutic target and different clinical trials are ongoing to evaluate the therapeutic effect of inhibitors of this pathway in renal cystic disease (56). Most of the studies so far reported have been performed in animal models for ADPKD. It will be interesting to test and confirm new therapeutic frontiers in other disease models. To this regard, the animal model we generated could represent a valuable tool to shed light on the molecular link between mTOR and cysts development and eventually to the identification of novel drug targets for renal cystic disease.

MATERIALS AND METHODS

Generation of *Ofd1*^{fl};*cre*^{Ksp} mice and PCR genotyping

Ofd1$^{fl/+}$ females (11) were crossed with *cre*^{Ksp} male mice containing 1.3 kb of the Ksp-cadherin promoter linked to the coding region of cre recombinase (23). Animals were genotyped for the presence of the floxed allele using the primers cre3 and cre4 to detect the *cre* gene as described by Ferrante *et al*. (11). All animal experimentation was performed under regulation of the Internal Ethical Committee and authorized by the Italian Ministry of Health.

RT–PCR and real-time PCR

Effective production of a deleted allele in the kidney was confirmed by RT–PCR (One-step system, Invitrogen) on kidney RNA or lung RNA, from wt and conditional mutants at P21, extracted with Trizol (Invitrogen), using primers Fsu1mcx and To-14020 (11). Quantification of *Ofd1* inactivation was assessed by real-time PCR on cDNA (SuperScript First-Strand, Invitrogen) synthesized from RNA from the kidney of P21 conditional mutants and controls. Primers used to amplify specifically the *Ofd1* wt allele were A (TGGCAGAC CACTTACAAAGATG), A′(AGACTGGATGAGGGGTTAA TC), B (CATTCCTGTTAGTATTTGGAGG) and B′ (GTGTT AGGAGGGTATGAACATG). A set of primers, GapdhF (*TCT TCTGGGTGGCAGTGAT*) and GapdhR (*TGCACCACCAAC TGCTTAGC*), that amplify the *Gapdh* gene were used as internal reference.

GFR assay

GFR measurements were performed on adult mice at P28, P35 and P45. A thiobutabarbital sodium (Inactin, Sigma-Aldrich) intraperitoneal injection (120 mg/kg body weight) was given as anesthetic. The animals were surgically prepared as follows: after tracheotomy, the left carotid artery and left jugular vein were cannulated with polyethylene tubing. The arterial catheter was then connected to a pressure transducer to monitor blood pressure and to take blood samples, while the venous catheter was connected to a syringe pump for saline infusion. After replacing surgical fluid loss with isotonic saline, the mice were given a priming dose of 10 μCi of [methoxy-^{3}H] inulin, followed by a maintenance infusion in isotonic saline containing 10 μCi/h at a rate of 0.4 ml/h. The bladder was cannulated with a PE 50 tube for urine collection. After a 60 min balance period, 30 min urine samples were collected. Blood samples were taken after each clearance period. A total of four urine and blood collections were made. GFR was calculated by standard methods.

SEM analysis

For SEM analysis, kidneys from P7 and P14 animals were fixed in Karnovsky fixative, postfixed with 1% osmium tetroxide in 0.1 M cacodylate buffer for 1 h at 4°C. Kidneys were sliced with a razor blade, dehydrated, dried with critical point-drying apparatus and mounted on aluminum stubs coated with palladium–gold using a cold sputter-coater. Analysis was performed with a Philips XL-20 microscope.

Histological and immunofluorescence assays

Isolated kidneys were fixed in 4% paraformaldehyde in PBS buffer at 4°C overnight. Hematoxylin–eosin stainings were performed on OCT (Kaltek) sections. For immunofluorescence

experiments, the OCT sections were incubated for 30 min with 0.1% BSA, 10% goat serum in TBS before incubation with the primary antibody at 4°C overnight. Sections were then washed with TBS and incubated with secondary Abs goat anti-mouse IgG conjugated to Cy3 and anti-rabbit IgG conjugated to FITC (Jackson ImmunoResearch). Stained sections were mounted with Vectashield (Vector Laboratories). The primary antibodies used were: anti-acetylated tubulin antibody (cat. no. T6793, Sigma-Aldrich), anti-NaPiII co-transporter (57), anti-PCNA (cat. no. sc-56, Santa Cruz Biotechnology), anti-Cleaved Caspase-3 (cat. no. 9661, Cell Signaling Technology, USA), anti-phosphoS6 (Ser235/236) (cat. no. 2211, Cell Signaling Technology, USA) and anti-Cre (cat. no. PBR-106C, Covance).

Staining for collecting ducts and distal tubules was performed with lectin from *Arachis hypogaea* (cat. no. L7759, Sigma-Aldrich) and with anti-Tamm–Horsfall glycoprotein (cat. no. CR2027SP, Europa Bioproducts) for detection of the thick ascending limb of Henle, according to manufacturer's instructions. PAS staining (cat. no. 395, Sigma-Aldrich) was performed on kidneys from $Ofd1^{fl}$;cre^{Ksp} mice at stage P23.

Microscopy was performed with a Zeiss Axioplan 2 microscope and a Leica TCS SP2 AOBS confocal microscope with a 63× Neofluor Pan-Apo 1.3 nm oil objective.

Immunoblot analysis

Western blot studies were performed in duplicate and at least two different animals were analyzed for each group. Kidneys were isolated and homogenized in RIPA buffer with protease and phosphatase inhibitor cocktails 1 and 2 (P2850 and P5726, Sigma-Aldrich). Western blot analysis on total proteins extracts was performed with antibodies for AKT (cat. no. 9272), phospho-AKT (Ser473) (cat. no. 9271), phospho-mTOR (Ser2448) (cat. no. 2971), phospho-P70S6K (Thr421/Ser424) (cat. no. 9204), S6 (cat. no. 2317) and phospho-S6 (cat. no. 2211) from Cell Signaling Technology (USA), mTOR (cat. no. KAP-ST220) and P70S6K (cat. no. KAP-CC035) from Stressgene Biotechnologies (CA, USA). Polyvinylidene difluoride membranes were used for Immunoblot (Millipore, USA) and ECL western blotting reagent (Amersham, UK) or Femto (Pierce, USA) for detection.

RNAi in MDCK cells

We designed two different pairs of DNA oligonucleotides (si254 and si1257) containing siRNA-expressing sequence targeting two regions of the canine OFD1 mRNA (XM_537958) using the software available at www.qiagen.com/GeneGlobe. We then cloned the annealed oligos into the expression vector pSuper (oligoengine). The cells were transfected with the Amaxa Nucleofactor system according to manufacturer's instructions (Cell Line Nucleofector®Kit L). RNA sequences were *GATCCCCGTGGTTTGGCCAAAGAAAATTCAAGAGATTTTCTTTGGCCAAACCAC* and *GATCCCCGGCCCAGATACGTGATTATTTCAAGAGAATAATCACGTATCTGGGCC* for si254 and si1257, respectively. The sequence for the scrambled oligo is *GATCCCCACTACCGTTGTTATAGGTGTTCAAGAGACACCTATAACAACGGTGTTTTTT*.

Rapamycin mice treatment and cystic index calculations

To evaluate the response to rapamycin treatment, mice received daily intraperitoneal injections of 2.5 mg/kg rapamycin dissolved in vehicle (10% DMSO, 10% ethanol and 80% saline) or vehicle alone. Rapamycin was administered starting at postnatal day 14 for a period of 10 days. For these experiments, three sets of animals (mutants and controls) from three different littermates were analyzed.

Representative images of hematoxylin–eosin-stained kidneys were acquired. A grid was placed over the images, and the cystic index was calculated as the percentage of grid intersection points that bisected cystic or non-cystic areas, as described previously (19).

SUPPLEMENTARY MATERIAL

Supplementary Material is available at *HMG* online.

ACKNOWLEDGEMENTS

We would like to thank Drs Sandro Banfi, Alessandra Boletta, Anna D'Angelo and Graciana Diez-Roux for helpful discussion and critical reading of the manuscript.

Conflict of Interest statement. None declared.

FUNDING

The generation of the *Ksp-Cre* line was supported by funding from the UT Southwestern O'Brien Kidney Research Core Center (NIH P30DK079328). This work was supported by grants from the Italian Telethon Foundation, the Polycystic Kidney Disease (PKD) Foundation (grant number 168G08a) and the European Union (grant HEALTH-F2-2007-201804) to B.F.

REFERENCES

1. Franco, B. (2008) The molecular basis of oral-facial-digital type I (OFDI) syndrome. In Epstein, J.C., Erickson, R.P. and Wynshaw-Boris, A. (eds), *Inborn Errors of Development*, 2nd edn, Oxford University Press, New York, Chapter 156, Vol. I, pp. 1379–1386.
2. Coll, E., Torra, R., Pascual, J., Botey, A., Ara, J., Perez, L., Ballesta, F. and Darnell, A. (1997) Sporadic orofaciodigital syndrome type 1 presenting as end-stage renal disease. *Nephrol. Dial. Transplant.*, **12**, 1040–1042.
3. Feather, S.A., Winyard, P.J., Dodd, S. and Woolf, A.S. (1997) Oral-facial-digital syndrome type 1 is another dominant polycystic kidney disease: clinical, radiological and histopathological features of a new kindred. *Nephrol. Dial. Transplant.*, **12**, 1354–1361.
4. Prattichizzo, C., Macca, M., Novelli, V., Giorgio, G., Barra, A. and Franco, B. (2008) Mutational spectrum of the oral-facial-digital type I syndrome: a study on a large collection of patients. *Hum. Mutat.*, **29**, 1237–1246.
5. Doege, T., Thuline, H., Priest, J., Norby, D. and Bryant, J. (1964) Studies of a family with the oral-facial-digital syndrome. *N. Engl. J. Med.*, **271**, 1073–1080.
6. Sabato, A., Fabris, A., Oldrizzi, L., Montemezzi, S. and Maschio, G. (1998) Evaluation of a patient with hypertension and mild renal failure in whom facial and digital abnormalities are noted. *Nephrol. Dial. Transplant.*, **13**, 763–766.
7. Macca, M. and Franco, B. (2009) The molecular basis of oral-facial-digital syndrome, type 1. *Am. J. Med. Genet.*, **151C**, 318–325.

8. Romio, L., Wright, V., Price, K., Winyard, P.J., Donnai, D., Porteous, M.E., Franco, B., Giorgio, G., Malcolm, S., Woolf, A.S. *et al.* (2003) OFD1, the gene mutated in oral-facial-digital syndrome type 1, is expressed in the metanephros and in human embryonic renal mesenchymal cells. *J. Am. Soc. Nephrol.*, **14**, 680–689.
9. Romio, L., Fry, A.M., Winyard, P.J., Malcolm, S., Woolf, A.S. and Feather, S.A. (2004) OFD1 is a centrosomal/basal body protein expressed during mesenchymal-epithelial transition in human nephrogenesis. *J. Am. Soc. Nephrol.*, **15**, 2556–2568.
10. Giorgio, G., Alfieri, M., Prattichizzo, C., Zullo, A., Cairo, S. and Franco, B. (2007) Functional characterization of the OFD1 protein reveals a nuclear localization and physical interaction with subunits of a chromatin remodeling complex. *Mol. Biol. Cell*, **18**, 4397–4404.
11. Ferrante, M.I., Zullo, A., Barra, A., Bimonte, S., Messaddeq, N., Studer, M., Dolle, P. and Franco, B. (2006) Oral-facial-digital type I protein is required for primary cilia formation and left–right axis specification. *Nat. Genet.*, **38**, 112–117.
12. Badano, J.L., Mitsuma, N., Beales, P.L. and Katsanis, N. (2006) The ciliopathies: an emerging class of human genetic disorders. *Annu. Rev. Genomics Hum. Genet.*, **7**, 125–128.
13. Bisgrove, B.W. and Yost, H.J. (2006) The roles of cilia in developmental disorders and disease. *Development (Cambridge, England)*, **133**, 4131–4143.
14. Sharma, N., Berbari, N.F. and Yoder, B.K. (2008) Ciliary dysfunction in developmental abnormalities and diseases. *Curr. Top. Dev. Biol.*, **85**, 371–427.
15. Hildebrandt, F. and Otto, E. (2005) Cilia and centrosomes: a unifying pathogenic concept for cystic kidney disease? *Nat. Rev. Genet.*, **6**, 928–940.
16. Yoder, B.K. (2007) Role of primary cilia in the pathogenesis of polycystic kidney disease. *J. Am. Soc. Nephrol.*, **18**, 1381–1388.
17. Deane, J.A. and Ricardo, S.D. (2007) Polycystic kidney disease and the renal cilium. *Nephrology (Carlton)*, **12**, 559–564.
18. Boletta, A. and Germino, G.G. (2003) Role of polycystins in renal tubulogenesis. *Trends. Cell Biol.*, **13**, 484–492.
19. Shillingford, J.M., Murcia, N.S., Larson, C.H., Low, S.H., Hedgepeth, R., Brown, N., Flask, C.A., Novick, A.C., Goldfarb, D.A., Kramer-Zucker, A. *et al.* (2006) The mTOR pathway is regulated by polycystin-1, and its inhibition reverses renal cystogenesis in polycystic kidney disease. *Proc. Natl Acad. Sci. USA*, **103**, 5466–5471.
20. Wahl, P.R., Serra, A.L., Le Hir, M., Molle, K.D., Hall, M.N. and Wuthrich, R.P. (2006) Inhibition of mTOR with sirolimus slows disease progression in Han:SPRD rats with autosomal dominant polycystic kidney disease (ADPKD). *Nephrol. Dial. Transplant.*, **21**, 598–604.
21. Tao, Y., Kim, J., Schrier, R.W. and Edelstein, C.L. (2005) Rapamycin markedly slows disease progression in a rat model of polycystic kidney disease. *J. Am. Soc. Nephrol.*, **16**, 46–51.
22. Zafar, I., Belibi, F.A., He, Z. and Edelstein, C.L. (2009) Long-term rapamycin therapy in the Han:SPRD rat model of polycystic kidney disease (PKD). *Nephrol. Dial. Transplant.*, **24**, 2349–2353.
23. Shao, X., Somlo, S. and Igarashi, P. (2002) Epithelial-specific Cre/lox recombination in the developing kidney and genitourinary tract. *J. Am. Soc. Nephrol.*, **13**, 1837–1846.
24. Hiesberger, T., Bai, Y., Shao, X., McNally, B.T., Sinclair, A.M., Tian, X., Somlo, S. and Igarashi, P. (2004) Mutation of hepatocyte nuclear factor-1beta inhibits Pkhd1 gene expression and produces renal cysts in mice. *J. Clin. Invest.*, **113**, 814–825.
25. Gresh, L., Fischer, E., Reimann, A., Tanguy, M., Garbay, S., Shao, X., Hiesberger, T., Fiette, L., Igarashi, P., Yaniv, M. *et al.* (2004) A transcriptional network in polycystic kidney disease. *EMBO J.*, **23**, 1657–1668.
26. Boletta, A. (2009) Emerging evidence of a link between the polycystins and the mTOR pathways. *Pathogenetics*, **2**, 6.
27. Sabers, C.J., Martin, M.M., Brunn, G.J., Williams, J.M., Dumont, F.J., Wiederrecht, G. and Abraham, R.T. (1995) Isolation of a protein target of the FKBP12–rapamycin complex in mammalian cells. *J. Biol. Chem.*, **270**, 815–822.
28. Shibazaki, S., Yu, Z., Nishio, S., Tian, X., Thomson, R.B., Mitobe, M., Louvi, A., Velazquez, H., Ishibe, S., Cantley, L.G. *et al.* (2008) Cyst formation and activation of the extracellular regulated kinase pathway after kidney specific inactivation of Pkd1. *Hum. Mol. Genet.*, **17**, 1505–1516.
29. Piontek, K., Menezes, L.F., Garcia-Gonzalez, M.A., Huso, D.L. and Germino, G.G. (2007) A critical developmental switch defines the kinetics of kidney cyst formation after loss of Pkd1. *Nat. Med.*, **13**, 1490–1495.
30. Lantinga-van Leeuwen, I.S., Leonhard, W.N., van der Wal, A., Breuning, M.H., de Heer, E. and Peters, D.J. (2007) Kidney-specific inactivation of the Pkd1 gene induces rapid cyst formation in developing kidneys and a slow onset of disease in adult mice. *Hum. Mol. Genet.*, **16**, 3188–3196.
31. Schwabe, G.C., Hoffmann, K., Loges, N.T., Birker, D., Rossier, C., de Santi, M.M., Olbrich, H., Fliegauf, M., Failly, M., Liebers, U. *et al.* (2008) Primary ciliary dyskinesia associated with normal axoneme ultrastructure is caused by DNAH11 mutations. *Hum. Mutat.*, **29**, 289–298.
32. Phillips, C.L., Miller, K.J., Filson, A.J., Nurnberger, J., Clendenon, J.L., Cook, G.W., Dunn, K.W., Overbeek, P.A., Gattone, V.H. 2nd and Bacallao, R.L. (2004) Renal cysts of inv/inv mice resemble early infantile nephronophthisis. *J. Am. Soc. Nephrol.*, **15**, 1744–1755.
33. Mokrzan, E.M., Lewis, J.S. and Mykytyn, K. (2007) Differences in renal tubule primary cilia length in a mouse model of Bardet–Biedl syndrome. *Nephron. Exp. Nephrol.*, **106**, e88–e96.
34. Donaldson, J.C., Dise, R.S., Ritchie, M.D. and Hanks, S.K. (2002) Nephrocystin-conserved domains involved in targeting to epithelial cell–cell junctions, interaction with filamins, and establishing cell polarity. *J. Biol. Chem.*, **277**, 29028–29035.
35. Benzing, T., Gerke, P., Hopker, K., Hildebrandt, F., Kim, E. and Walz, G. (2001) Nephrocystin interacts with Pyk2, p130(Cas), and tensin and triggers phosphorylation of Pyk2. *Proc. Natl Acad. Sci. USA*, **98**, 9784–9789.
36. Nurnberger, J., Bacallao, R.L. and Phillips, C.L. (2002) Inversin forms a complex with catenins and N-cadherin in polarized epithelial cells. *Mol. Biol. Cell*, **13**, 3096–3106.
37. Taulman, P.D., Haycraft, C.J., Balkovetz, D.F. and Yoder, B.K. (2001) Polaris, a protein involved in left–right axis patterning, localizes to basal bodies and cilia. *Mol. Biol. Cell*, **12**, 589–599.
38. Yoder, B.K., Hou, X. and Guay-Woodford, L.M. (2002) The polycystic kidney disease proteins, polycystin-1, polycystin-2, polaris, and cystin, are co-localized in renal cilia. *J. Am. Soc. Nephrol.*, **13**, 2508–2516.
39. Murcia, N.S., Richards, W.G., Yoder, B.K., Mucenski, M.L., Dunlap, J.R. and Woychik, R.P. (2000) The Oak Ridge Polycystic Kidney (orpk) disease gene is required for left–right axis determination. *Development*, **127**, 2347–2355.
40. Lehman, J.M., Michaud, E.J., Schoeb, T.R., Aydin-Son, Y., Miller, M. and Yoder, B.K. (2008) The Oak Ridge Polycystic Kidney mouse: modeling ciliopathies of mice and men. *Dev. Dyn.*, **237**, 1960–1971.
41. Pazour, G.J., Dickert, B.L., Vucica, Y., Seeley, E.S., Rosenbaum, J.L., Witman, G.B. and Cole, D.G. (2000) Chlamydomonas IFT88 and its mouse homologue, polycystic kidney disease gene tg737, are required for assembly of cilia and flagella. *J. Cell Biol.*, **151**, 709–718.
42. Brown, N.E. and Murcia, N.S. (2003) Delayed cystogenesis and increased ciliogenesis associated with the re-expression of polaris in Tg737 mutant mice. *Kidney Int.*, **63**, 1220–1229.
43. Watnick, T. and Germino, G. (2003) From cilia to cyst. *Nat. Genet.*, **34**, 355–356.
44. Cogswell, C., Price, S.J., Hou, X., Guay-Woodford, L.M., Flaherty, L. and Bryda, E.C. (2003) Positional cloning of jcpk/bpk locus of the mouse. *Mamm. Genome*, **14**, 242–249.
45. Maisonneuve, C., Guilleret, I., Vick, P., Weber, T., Andre, P., Beyer, T., Blum, M. and Constam, D.B. (2009) Bicaudal C, a novel regulator of Dvl signaling abutting RNA-processing bodies, controls cilia orientation and leftward flow. *Development*, **136**, 3019–3030.
46. Hasumi, Y., Baba, M., Ajima, R., Hasumi, H., Valera, V.A., Klein, M.E., Haines, D.C., Merino, M.J., Hong, S.B., Yamaguchi, T.P. *et al.* (2009) Homozygous loss of BHD causes early embryonic lethality and kidney tumor development with activation of mTORC1 and mTORC2. *Proc. Natl Acad. Sci. USA*, **106**, 18722–18727.
47. Hasumi, H., Baba, M., Hong, S.B., Hasumi, Y., Huang, Y., Yao, M., Valera, V.A., Linehan, W.M. and Schmidt, L.S. (2008) Identification and characterization of a novel folliculin-interacting protein FNIP2. *Gene*, **415**, 60–67.
48. Chen, J., Futami, K., Petillo, D., Peng, J., Wang, P., Knol, J., Li, Y., Khoo, S.K., Huang, D., Qian, C.N. *et al.* (2008) Deficiency of FLCN in mouse kidney led to development of polycystic kidneys and renal neoplasia. *PLoS ONE*, **3**, e3581.
49. Lin, F., Hiesberger, T., Cordes, K., Sinclair, A.M., Goldstein, L.S., Somlo, S. and Igarashi, P. (2003) Kidney-specific inactivation of the KIF3A

subunit of kinesin-II inhibits renal ciliogenesis and produces polycystic kidney disease. *Proc. Natl Acad. Sci. USA*, **100**, 5286–5291.
50. Potter, C.J., Huang, H. and Xu, T. (2001) Drosophila Tsc1 functions with Tsc2 to antagonize insulin signaling in regulating cell growth, cell proliferation, and organ size. *Cell*, **105**, 357–368.
51. Potter, C.J., Pedraza, L.G., Huang, H. and Xu, T. (2003) The tuberous sclerosis complex (TSC) pathway and mechanism of size control. *Biochem. Soc. Trans.*, **31**, 584–586.
52. Inoki, K., Li, Y., Zhu, T., Wu, J. and Guan, K.L. (2002) TSC2 is phosphorylated and inhibited by Akt and suppresses mTOR signalling. *Nat. Cell Biol.*, **4**, 648–657.
53. Zhou, J., Brugarolas, J. and Parada, L.F. (2009) Loss of Tsc1, but not Pten, in renal tubular cells causes polycystic kidney disease by activating mTORC1. *Hum. Mol. Genet.*, **18**, 4428–4441.
54. DiBella, L.M., Park, A. and Sun, Z. (2009) Zebrafish Tsc1 reveals functional interactions between the cilium and the TOR pathway. *Hum. Mol. Genet.*, **18**, 595–606.
55. Hartman, T.R., Liu, D., Zilfou, J.T., Robb, V., Morrison, T., Watnick, T. and Henske, E.P. (2009) The tuberous sclerosis proteins regulate formation of the primary cilium via a rapamycin-insensitive and polycystin 1-independent pathway. *Hum. Mol. Genet.*, **18**, 151–163.
56. Serra, A.L., Kistler, A.D., Poster, D., Struker, M., Wuthrich, R.P., Weishaupt, D. and Tschirch, F. (2007) Clinical proof-of-concept trial to assess the therapeutic effect of sirolimus in patients with autosomal dominant polycystic kidney disease: SUISSE ADPKD study. *BMC Nephrol.*, **8**, 13.
57. Custer, M., Lotscher, M., Biber, J., Murer, H. and Kaissling, B. (1994) Expression of Na-P(i) cotransport in rat kidney: localization by RT–PCR and immunohistochemistry. *Am. J. Physiol.*, **266**, F767–F774.